JOURNAL OF MATERIALS SCIENCE 14 (1979) 1827–1837

Experimental and theoretical investigations on morphological changes of γ' precipitates in Ni-Al single crystals during uniaxial stress-annealing

TORU MIYAZAKI, KOZO NAKAMURA*, HIROTARO MORI
Department of Metallurgical Engineering, Nagoya Institute of Technology, Nagoya, Japan

Influences of the external tension and compression on the morphological changes of γ' precipitates during coarsening in an Ni–15 at. % Al single crystal were experimentally investigated, and theoretical evalutions on the energetically favourable shape and its orientation were also derived based upon the anisotropic elasticity theory. The shape transformation with growth in size is experimentally found to follow the sequence: cuboid → rod → plate, under all annealing conditions, i.e. compression-annealing, tension-annealing and external stress-free annealing. However, the external stresses give preferential orientation to such microstructures. The tension of the [0 0 1] direction aligns the rods and plates along the tension axis, while the compression aligns them on a plane perpendicular to the compression axis. Theoretical evaluations based upon the anisotropic elasticity for the energetically favourable shapes and orientations of γ' are consistent with experimental results except in the appearance of rods after compression-annealing. This discrepancy is understood by a conception that the shape transformation is influenced not only by energetics in the elastic strain and interfacial energies, but also by elastic interaction energy.

1. Introduction

The influence of external stress on the orientation of precipitates has been found in several alloys. For instance, Fe_8N in Fe–N alloy [1], γ'' in 718 alloy [2], and Au in Fe–Mo–Au alloy [3], which are all plate-like in shape and are nucleated on the (0 0 1) plane of the matrix when the tensile stress acts uniaxially on the [0 0 1] direction of the matrix, while θ in Al–Cu alloy [4], $ZrH_{1.5}$ in Zr–H alloy [5] and Ti-hydride in Ti–H alloy [6] are formed on the (1 0 0) and (0 1 0) planes parallel to the tensile axis. All the experimental results described above have briefly been accounted for by an understanding that the precipitates are produced on crystal plane of the matrix where the elastic strain associated with the precipitate can be relaxed by the external stress, and calculations based upon the anisotropic elasticity theory for energetically favourable orientations of the precipitates have not been derived. Tien and Copley [7] observed the electron microscopic structure of γ' precipitates in the Udimet 700 single crystal annealed under external stress, and found that the external stress influenced not only the orientation but also the shape of the γ' precipitates. According to them, the plate-like γ' perpendicular to the tensile axis and the rods parallel to the compression axis are stable configurations. To understand these results, Pineau [8] derived numerical expressions for energetically favourable shapes and orientations of the precipitates using the isotropic elasticity theory. However, the calculations should be derived on the basis of the anisotropic elasticity theory for such anisotropic media.

*Formerly at the Graduate School of Nagoya Institute of Technology. Present address: Komatsu Ltd, Tokyo, Japan.

0022–2461/79/081827–11 $03.10/0

As mentioned above, the influences of the external stress on the orientation and shape of precipitates in an anisotropic matrix have not so far been evaluated to our knowledge. In the present we shall first show the experimental results on the orientation and shape changes of γ' precipitates in an Ni–15 at.% Al single crystal during uniaxial stress-annealing, and then calculate the anisotropic elastic strain energies for ellipsoidal precipitates contained in an externally stressed matrix as functions of shape, size and orientation of the ellipsoids using the method of Eshelby [10]. The Ni–Al alloy was chosen because the elastic constants and the interfacial energy of conjugating phases have been clarified by many examinations which were carried out because of the basic alloy system of the super heat-resisting alloys.

2. Alloy preparation and experimental procedure

2.1. Preparation of single crystals and heat-treatment

An Ni–15 at.% Al alloy was prepared using 99.9% pure Ni and 99.99% pure Al. The alloy was induction-melted in an atmosphere of argon, and then forged into 9 mm diameter rods at room temperature. These were used as the base material for the single crystals. The single crystals the longitudinal direction of which was [0 0 1], were prepared from the rod by the Bridgman method. Chemical composition of the single crystals was analysed to be Ni–15.06 at.% Al by EPMA measurement. The rods were carefully lathed and then chemically polished for about 0.1 mm depth from the side surface to form specimens of 4 mm diameter.

The single crystals were held at 1200° C for 30 min in a vacuum vertical electric furnace and then drop-quenched into iced brine. After pre-ageing at 750° C for 24 h in vacuum, the specimens were annealed in vacuum at the same temperature for prescribed annealing times under uniaxially tensile or compressive stresses of 147 MPa along the [0 0 1] direction using a creep testing machine. In the ordinary creep machine only tensile loading may be applied, but in the present study an apparatus was devised, in which compressive stress could be applied to the test pieces without changing the loading system of the machine. A stress-free annealing was also conducted on a separate single crystal placed by the stressed specimen in the furnace of the creep testing machine.

2.2. Metallographic examination

The shapes and distributions were mainly examined by electron microscopy for the thin foils and the chromium shadowing carbon replicas. Thin foils for TEM were prepared by electric polishing in phosphoric–chromic acid solution at room temperature. Electron microscopic observations were carried out on the (1 0 0) or (0 1 0) planes of the side face and the (0 0 1) plane of the cross-section of the specimens. The microscope (JEM 200A) was operated at 100 kV for the replicas and at 200 kV for the thin foils.

2.3. Measurement of elastic constants

The elastic stiffness constants of the matrix and the γ' phases at the annealing temperature of 750° C are needed to calculate the elastic strain energies arising from the lattice misfit between the conjugating phases. Since the elastic constants of the γ' phase (Ni_3Al) have already been examined [11, 12] measurements were made only for the matrix. An Ni–13.5 at.% Al single crystal, whose Al content was nearly equal to the solution-limit of Al at 750° C in the equilibrium phase diagram [13], was used for the measurement of the elastic constants of the matrix by means of the ultrasonic pulse method, details of which were given in our previous paper [14].

3. Experimental results

3.1. Morphological changes of γ' precipitates during stress-annealing

The pre-ageing at 750° C for 24 h gives rise to periodic arrays, along the ⟨1 0 0⟩ cube directions, of coherent cuboids with distinct interfaces parallel to the {1 0 0} family planes of the matrix, as shown in Fig. 1. The average edge length of the cuboids is about 70 nm. It is remarkable that in the distribution of γ', the cuboids are not uniformly distributed, but are localized in rows. The causes of this arrangement will be discussed in Section 5.

Fig. 2a, b and c are the replica micrographs of the (1 0 0) side surfaces of the single crystals annealed at 750° C for 160 h, after pre-ageing, under the conditions of no external stress, tension and compression of 147 MPa, respectively. As is clearly shown in the figures, most of the precipitates which were cuboid before annealing are transformed to rods and/or plates. The precipitates seem to be aligned along the three ⟨1 0 0⟩ cube directions in same proportions as when the specimen was annealed without external stress. For the

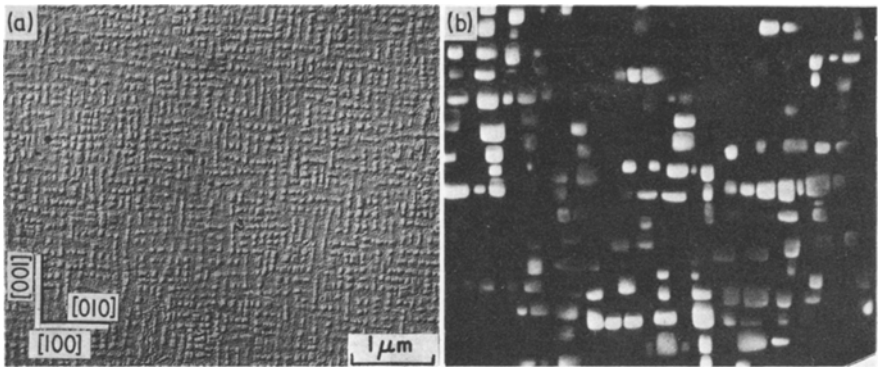

Figure 1 A replica micrograph (a) and a transmission electron dark-field image (b) taken using 100 super lattice reflection spots for γ' precipitates in an Ni–15 at.% Al single crystal aged at 750° C for 24 h, showing the γ' cuboids aligned along the ⟨1 0 0⟩ cube directions.

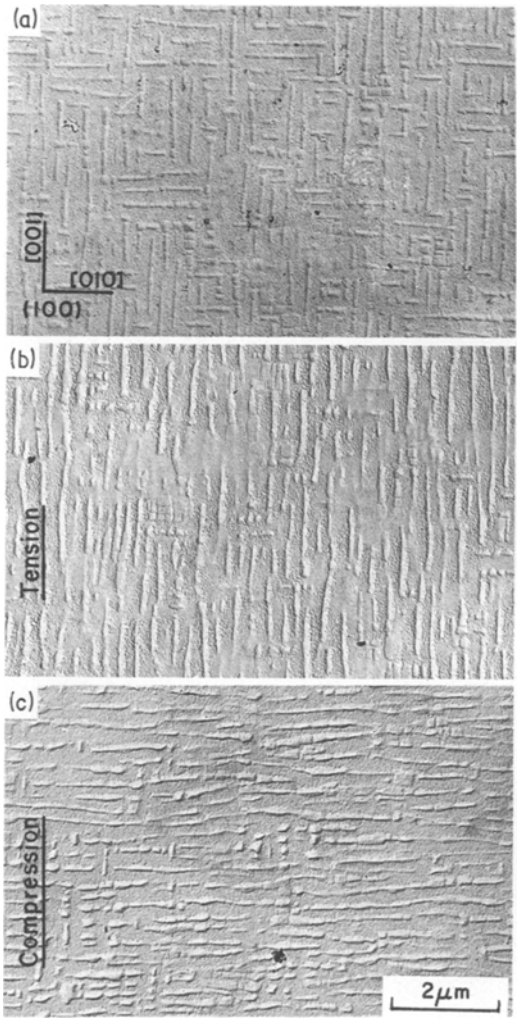

Figure 2 The replica microphotograph of the (1 0 0) side of the specimens annealed at 750° C for 160 h, after preageing, without external stress (a), and with uniaxial tension (b), and compression (c), of 147 MPa, showing clearly the different orientations of γ' precipitates with the different external stresses.

stress-annealing, however, the influence of external stresses can be seen clearly in orientation; the rods tend to be parallel to the stress direction for the case of tension-annealing, but normal to this direction when the specimens undergo compression-annealing. These results are not consistent with those of Tien and Copley's [7] presented in Section 1.

Transmission electron microscope observations were also made. Fig. 3a and b, taken from the (1 0 0) thin foils prepared from the slivered single crystals, show the shape development of γ' during stress-free annealing. Most of the γ' precipitates in Fig. 3a are recognized as plate-like or rod-like. The final stable shape of γ' is considered to be plate-like, because the plates increase in number with growth in size. Therefore, the sequence of shape changes of γ' is: cuboid → rod → plate with growth in size. This fact coincides with Chou *et al.*'s results for the shape development of precipitates in a Cu–Ni–Cr modulated structure alloy [15].

The influence of uniaxial tension on the arrangement of γ' is clearly revealed in Fig. 4, where (a) and (a′) show the microstructures of the cross (0 0 1) and side (1 0 0) cube planes, respectively. This pair of photographs were taken as evidence of anisotropic arrangement in three dimensions in the γ'-orientation. From the figure, preferential orientation due to the external stress can easily be seen to be parallel to the tension axis. A longer ageing time tends to transform the rod-like γ' to plates and gives rise to a mixed structure of fairly well developed plates and rods, as is seen in Fig. 4b and b′.

For the case of compression-annealing, the cuboids mostly change to rods normal to the stress

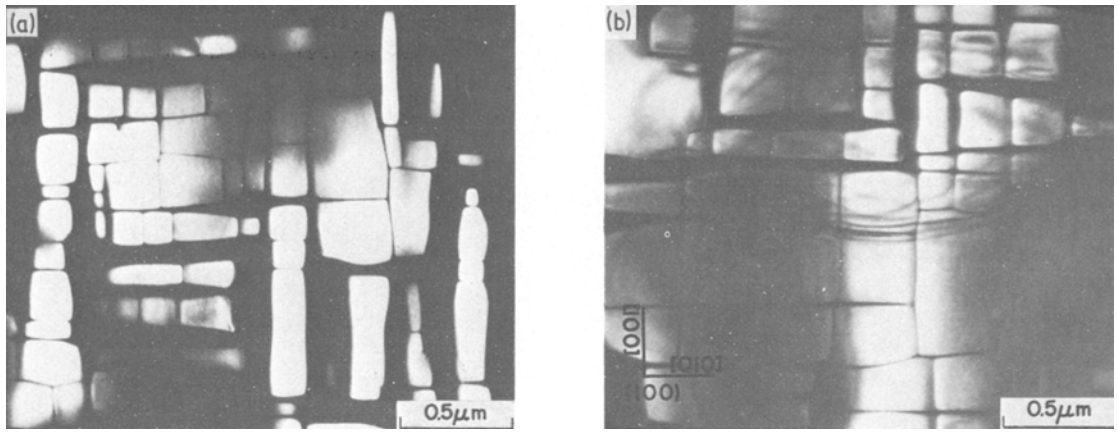

Figure 3 Development of the morphology of γ' precipitates with the progress of stress-free annealing. (a) 750° C for 160 h, (b) 750° C for 280 h. Beam direction = [1 0 0], g = 0 0 1.

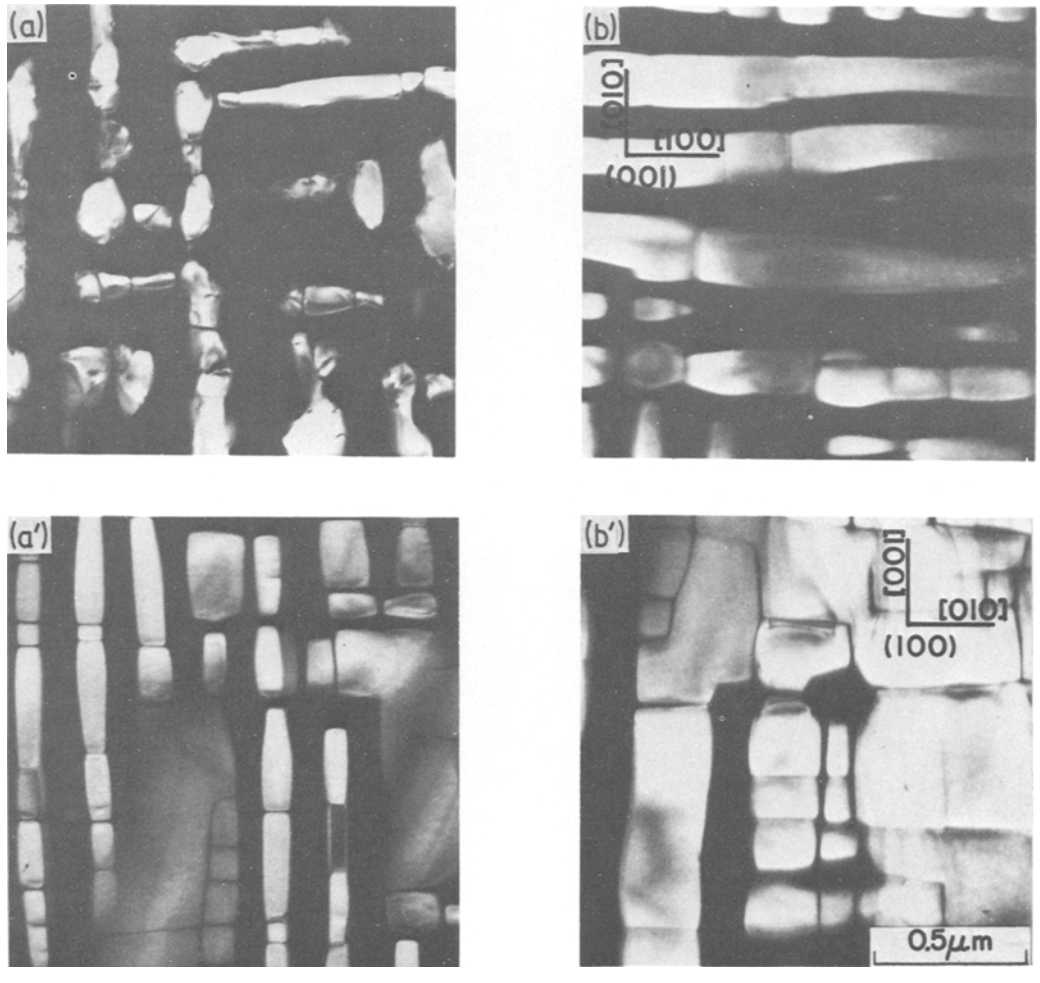

Figure 4 Dark-field images of specimens annealed at 750° C for 160 h (a) and (a′), and for 280 h (b) and (b′) under a tensile stress of 147 MPa along the [0 0 1] direction, showing cubic non-equivalent microstructures caused by the external stress (a) and (b) show transverse (0 0 1) planes, and (a′) and (b′) are of the (1 0 0) side plane.

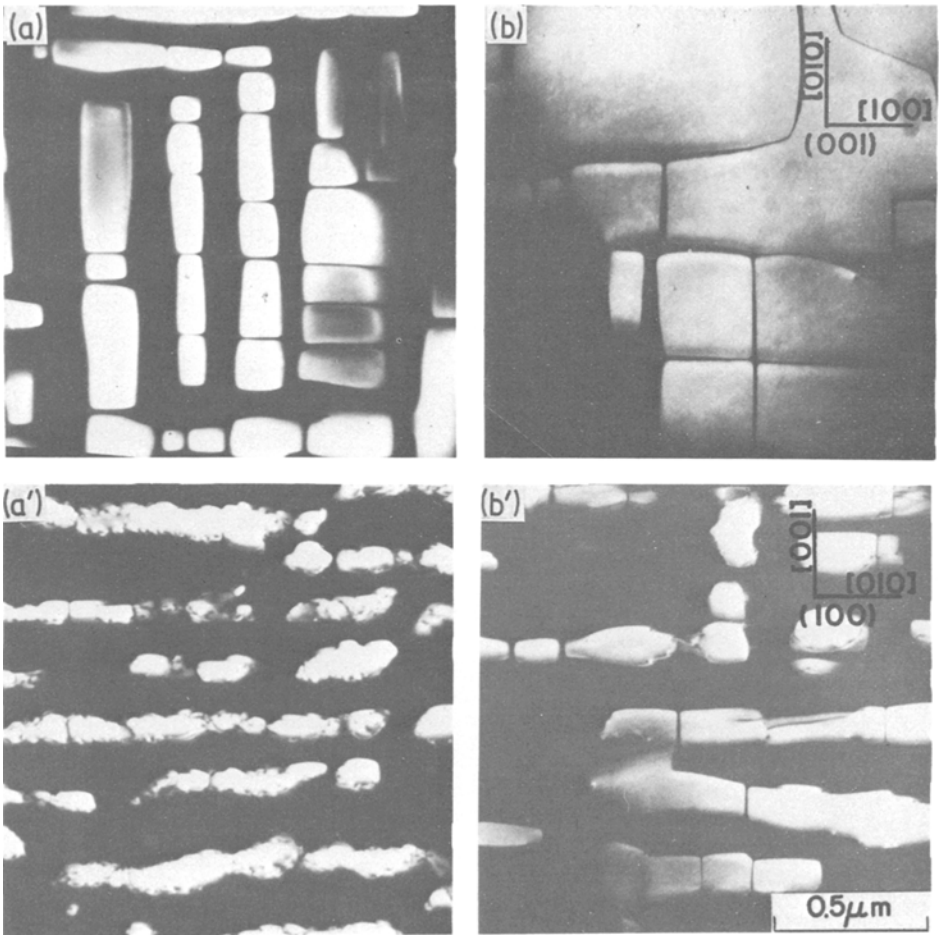

Figure 5 The influences of compressive stress along the [0 0 1] direction of 147 MPa on the morphology of γ' in specimens annealed at 750° C for 160 h (a) and (a'), and for 280 h (b) and (b'). Signs with and without primes are identical to those of Fig. 4.

axis during annealing for 160 h as seen in Fig. 5a and a' and some of them then become plate-like as seen in Fig. 5b and b'.

Consequently, a general view of the morphological changes is expressed as follows: shape transformation occurs in the sequence, cuboid → rod → plate, with progress of annealing, notwithstanding different annealing conditions, and the external stress causes the preferential orientations of the rods and plates.

3.2. Elastic constants

Temperature dependencies of Young's moduli of γ' (Ni_3Al) which have been measured by Davies and Stoloff [12] and Ni–13.5 at % Al polycrystalline alloy which was experimentally obtained in the present work, are shown in Fig. 6. The γ' phase is sure to be elastically harder than the matrix at an annealing temperature of 750° C. The elastic constants, C_{11}, C_{12} and C_{44} are required, instead of the Young's modulus, to calculate the energetically favourable shapes and orientations of the γ' precipitates in the anisotropic matrix. However, having not been measured yet as far as we know, the high-temperature stiffness constants of the γ' and matrix phases were estimated approximately from the temperature dependencies of Young's moduli, $E_{750° C}/E_{RT}$, shown in Fig. 6. Assuming the elastic anisotropy of the γ' phase to be constant for a temperature range up to 750° C, the stiffness constants of γ' at the high temperature were calculated by multiplying a factor of $E_{750° C}/E_{RT}$ by the room temperature stiffness constants which had already been obtained by Ono and Stern [16], to be $C_{11} = 19.8 \times 10^4$, $C_{12} = 12.7 \times 10^4$ and $C_{44} = 11.8 \times 10^4$ MN m^{-2}. If the elastic anisotropy of pure Ni [17] is assumed to be equal to that of Ni– 13.5 at. % Al alloy, the

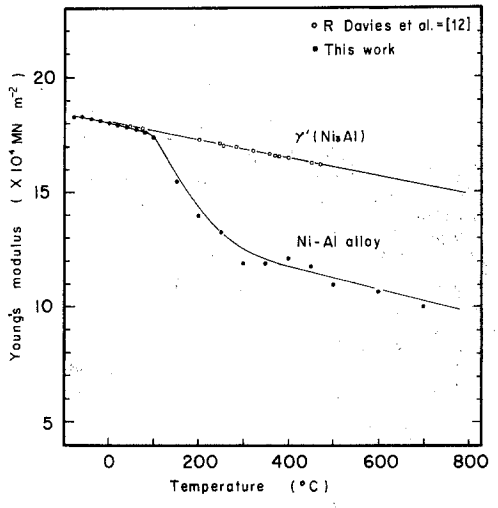

Figure 6 Temperature dependence of Young's moduli of an Ni–13.5 at. % Al polycrystalline alloy and of the Ni_3Al single phase which was measured by Davies and Stoloff [12].

stiffness constants of the matrix may be in the same way as for the γ' phase. These elastic constants may contain some uncertainties. Nevertheless, they are considered to be a good enough approximation for calculating the energetically favourable shape and orientation of the precipitates, because the theoretically given stable shape is not replaced by other shapes, provided that the Young's moduli of the γ' and matrix phases are not reversed. The elastic stiffness constants used in the calculation are given in Table I.

TABLE I Numerical values used for the calculation of the total elastic energy E. The interfacial energy γ_s is taken from Ardell's work [21]

Elastic constants of matrix at 750° C (10^4 MN m^{-2})	
C_{11}	11.24
C_{12}	6.27
C_{44}	5.69
Elastic constants of γ' at 750° C (10^4 MN m^{-2})	
C^*_{11}	16.66
C^*_{12}	10.65
C^*_{44}	9.92
Stress free strain, e^{T*}	0.005 63
External stress (MPa), σ^A	147
Interfacial energy (Jm^{-2}) γ_s	1.42×10^{-2}

4. Theoretical evaluation of energetically favourable orientations and shapes of the γ' precipitates in an externally stressed anisotropic matrix

Two energy terms, elastic strain energy and interfacial energy, of coherent two-phase mixtures yield the most energetically favourable configurations to each precipitate. The elastic strain energy of a precipitate is first considered.

The elastic strain energy (E_t) of an elipsoid inclusion E_t in a externally stressed solid consists of three types of energy [9]; an elastic strain energy due to the lattice misfit between the matrix and precipitate, which exists even in the case of external stress free, E_{incl}, an interaction energy between the external stress and the elastic strain field, E_{int}, and disturbance of the external stress caused by the inhomogeneous inclusion, E_{inh}.

$$E_t = E_{incl} + E_{int} + E_{inh} \quad (1)$$

According to Eshelby [9, 10], these energies per unit volume of precipitate contained in an infinite matrix are given by following equation, when the ellipsoidal approximation for the shape of precipitate is employed.

$$E_{incl} = -(1/2)\,\sigma^I_{ij}\,e^{T*}_{ij} \quad (2a)$$

$$E_{int} = -\sigma^A_{ij}\,e^T_{ij} \quad (2b)$$

$$E_{inh} = -(1/2)\,\sigma^A_{ij}\,e^{Th}_{ij} \quad (2c)$$

Here, the notations are as follows; σ^A_{ij} is an applied stress which is negative for the compression and positive for the tension, σ^I_{ij} is a stress inside the ellipsoidal inclusion and e^{T*}_{ij} is the eigenstrain (transformation strain) of precipitate, representing $e^{T*}_{11} = e^{T*}_{22} = e^{T*}_{33} = \sigma = (a_p - a_m)/a_m$ when the strains are of pure dilatation (a_m and a_p are lattice parameters of non-constrained matrix and precipitate, respectively). e^T_{ij} is a transformation strain of the equivalent ellipsoid having the same elastic constants as the matrix but different size from the inclusion. e^{Th}_{ij} is an additional transformation strain of the equivalent ellipsoid, which is introduced to restore the disturbance of elastic field caused by the action of external stress on the elastically inhomogeneous media.

When the shape of inclusion is ellipsoidal, the stress σ^I_{ij} is proved to be constant inside the inclusion even for anisotropic media by Kinoshita *et*

al. [18]. Therefore, Equations 2a to 2c introduced by Eshelby [9, 10] for the isotropic media are also applicable to the anisotropic media. The stress σ_{ij}^{I} is related to the constrained strain (total strain) e_{kl}^{c} of the inclusion as in Equation 3 which has been obtained by considering the equivalency of the stress and strain of the inhomogeneous inclusion and the equivalent homogeneous inclusion [9].

$$\sigma_{ij}^{I} = C_{ijkl}(e_{kl}^{c} - e_{kl}^{T}) = C_{ijkl}^{*}(e_{kl}^{c} - e_{kl}^{T*}), \quad (3)$$

where C_{ijkl} and C_{ijkl}^{*} are elastic constants of the matrix and inclusion, respectively. The relationship between the equivalent transformation strain e_{kl}^{T} and the constrained strain e_{ij}^{c} is given by Equation 4.

$$e_{ij}^{c} = S_{ijkl}e_{kl}^{T}. \quad (4)$$

S_{ijkl}, a so-called Eshelby tensor [9], has been expressed as $S_{ijkl} = (1/4)C_{jlmn}\,\bar{G}_{ijkl}$, and $\bar{G}_{ijkl}$ has been concretely given as a function of the aspect ratio of an ellipsoid by Lin and Mura [19]. Therefore, if the eigenstrain e_{kl}^{T*} is experimentally given, e_{ij}^{c}, e_{ij}^{T} and σ_{ij}^{I} are found from the simultaneous Equations 3 and 4. Further, e_{ij}^{Th} is found by simultaneously solving the following linear equations instead of Equations 3 and 4;

$$C_{ijkl}(e_{kl}^{A} + e_{kl}^{ch} - e_{kl}^{Th}) = C_{ijkl}^{*}(e_{kl}^{A} + e_{kl}^{ch}) \quad (5)$$

$$e_{ij}^{ch} = S_{ijkl}e_{kl}^{Th} \quad (6)$$

where e_{kl}^{A} is the strain defined by the Hooke's law $\sigma_{ij}^{A} = C_{ijkl}\,e_{kl}^{A}$, and e_{ij}^{ch} is the elastic strain of the inclusion caused by the external stress. Equation 5 is introduced by the same consideration as Equation 3 [9].

Since the Ni–Al alloy of the present work has an elastic anisotropy factor greater than unity, the revolution axes a and c of ellipsoid should be consistent with the ⟨1 0 0⟩ cube directions of the crystal [20]. Therefore, a calculation was performed to relate the a-axis with the 1-axis and the c-axis with the 3-axis.

Another energy changeable with the shape of inclusion is the interfacial energy, E_{surf}. It is presented in Equation 7 as functions of size and aspect ratio of the ellipsoid.

$$E_{surf} = \gamma_s \pi r^2 P^{-(2/3)}[2 + F(P)] \quad (7)$$

$$P < 1; F(P) = [2P^2/\sqrt{(1-P^2)}] \log\{[1 + \sqrt{(1-P^2)}]/P\}$$

$$P = 1; F(P) = 2$$

$$P > 1; F(P) = [2P^2/\sqrt{(P^2-1)}] \cdot \tan^{-1}\sqrt{(P^2-1)},$$

where γ_s is the interfacial energy of inclusion per unit area, P is the aspect ratio c/a and r is a radius of spherical particle whose volume is same as that of the ellipsoid.

Consequently, the total energy E, of an ellipsoid of revolution is given by Equation 8.

$$E = E_t(4/3)\pi r^3 + E_{surf} \quad (8)$$

All the numerical values used in the calculation are summarized in Table I. The eigenstrain e^{T*} at 750° C was evaluated from the lattice constants of an Ni solid solution containing 13.5 at.% Al, measured by X-ray diffraction in the present work and of the Ni_3Al single phase [22].

The results of numerical calculation are now presented. Fig. 7 shows shape dependencies of the total elastic strain energy E_t for the cases of $\sigma^{A} = 0$ and ± 147 MPa. The aspect ratio $c/a = 1$ corresponds to a sphere, and the right-and left-hand sides from the centre mean needle-shaped and plate-shaped ellipsoids, respectively. The solid and dotted lined in Fig. 7 show the energy changes

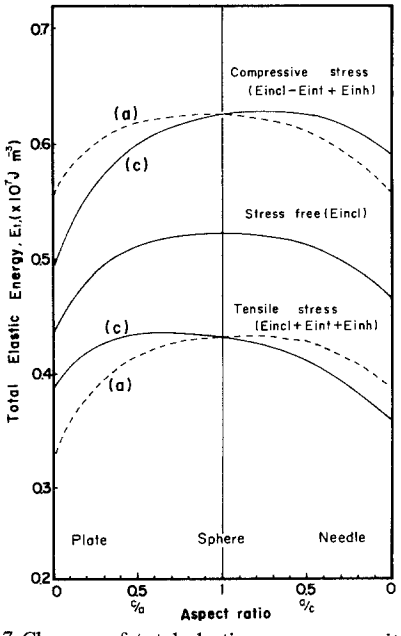

Figure 7 Changes of total elastic energy per unit volume of ellipsoid with aspect ratio, showing the most energetically favourable shape to be plate-like for all annealing conditions, but different orientations with different external stresses. The solid and dotted lines represent the enrgy changes for external stress acting along the c- and a-axis, respectively, of the ellipsoid of revolution.

for external stress parallel to the c- and a-axes, respectively, of ellipsoids of revolution. From Fig. 7 the most energetically favourable shape is found to be the plate in all three annealing conditions, but the broad faces of the plates are oriented perpendicular to the stress axis for the compression-annealing, and parallel to it for the tension-annealing.

On the basis of isotropic elasticity theory, a numerical evaluation for the stable shapes was also derived for the present alloy using Eshelby's equation (Equation 2) under the conditions of Poisson's ratio $\nu = 0.3$ and Young's moduli 10.0×10^4 MN m^{-2} for the matrix and 15.1×10^4 MN m^{-2} [12] for the γ' phases. The calculation, however, gave a sphere as the energetically favourable shape for all three annealing conditions. This is obviously inconsistent with the experimental shape transformation. Therefore, the isotropic elasticity theory is insufficient to explain precipitate morphology in anisotropic crystals such as Ni-base alloys.

Relationships between the total energy E, aspect ratio and size of ellipsoid for the case of $\sigma^A = 0$ are given in Fig. 8. The ordinate is normalized by the total energy of the sphere. It is clearly found that, when the size is small, such as $r = 40$ nm, the minimum total energy is realized at $c/a = 1$, i.e. corresponding to a sphere, but with increase in radius the energetically favourable shape

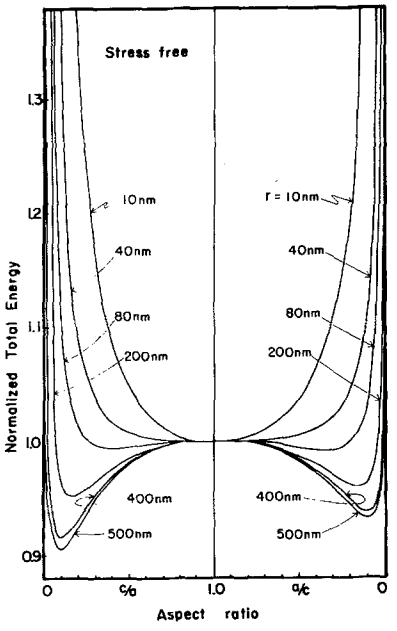

Figure 8 Relationships between the total energy E, the aspect ratio and the radius of ellipsoid for the case of external stress-free annealing.

becomes rod-like ($a/c = 0.6$) at a medium size $r = 80$ nm although the energetic priority is small; the final stable shape appears as a plate, when the size is large, over $r = 200$ nm. Such theoretically given shape transformations are experimentally confirmed from the microstructures in Fig. 3.

The effects of tensile stress on the energetically favourable orientation and shape are given in Fig. 9. The solid and dotted lines have the same meaning as in Fig. 6. The rod-like shape parallel to the tension axis has transitory minimum energy when the radius is small, such as $r = 40$ or 80 nm, and then the plates along the axis becomes more favourble with increase in radius, as shown for the case of $r = 400$ nm. By computations the energetic favourability of the plate was confirmed to become more distinct with further increase in size. Thus, theoretically given orientations of rod- and plate-shaped γ' agree with the experimental ones, as clearly recognized from Fig. 4. The energy changes for the compression-annealing ($\sigma^A = -147$ MPa) are shown in Fig. 10. It is clearly found from the figure that the compression stress forces the plates to be aligned perpendicular to the stress axis. This theoretical orientation is consistent with experimental results (see Fig. 5).

5. Discussion

As above described, the anisotropic elasticity theory explains well the practical morphology changes of γ' precipitates during stress-annealing and stress-free annealing. However, an inconsistency between the theoretical and experimental results is recognized. According to the energetic evaluation for the case of compression-annealing, the plate is always more favourable than the rod, for any size of inclusion (see Fig. 10). Therefore, the plates should be directly produced from the cuboidal γ' without passing through the rod shape. In the microscopic observation, however, the rod-shaped γ' precipitates are obviously observed as an intermediate in the transformation sequence (see Fig. 5). We consider that such a contradiction may arise from disregarding the alignments of inclusions enforced by the elastic interactions among the inclusions. This influence of the elastic interactions on the shape transformation is discussed. Khachaturyan [23] dealt with a theoretical evaluation on the energetic priorities for several types of three-dimensional arrangements of spherical inclusions, and found that the cubic arrays of inclusions along three ⟨1 0 0⟩ directions were the ener-

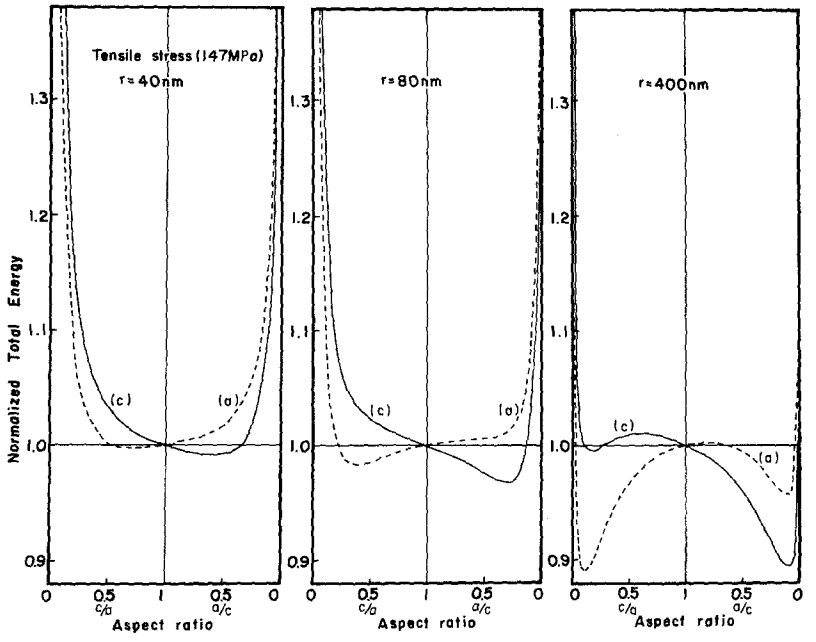

Figure 9 Changes in total energy E with aspect ratio for radius of 40, 80 and 400 nm of inclusions under a tensile stress of 147 MPa.

getically favourable for alloys where the matrix had an elastic anisotropy parameter greater than unity. Similiar results have been obtained by Yamauchi and co-worker [24, 25]. According to these authors, who developed it more generally, the elastic interaction energy, $E_{\alpha\beta}$ between two spherical particles α and β contained in the highly anisotropic matrix such as Cu, is as represented in Fig. 11. From it, the most energetically favourable position of a neighbouring particle is found to be slightly away from the original sphere along the ⟨1 0 0⟩ cube direction. The minimum value of the potentials is recognized to be about 10% E_{self} ($= VE_{\text{incl}}$, where V is the volume of inclusion).

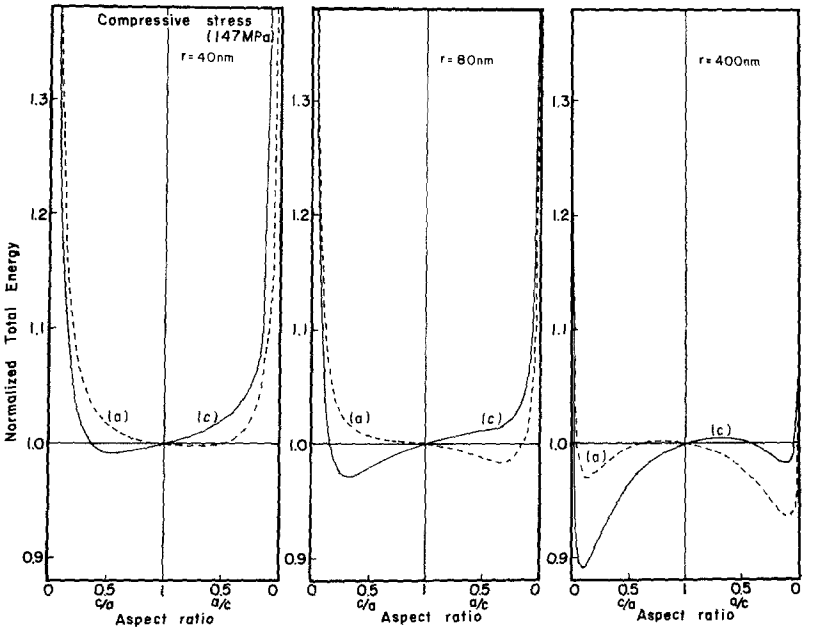

Figure 10 Changes in the total energy E with aspect ratio under a compressive stress of 147 MPa.

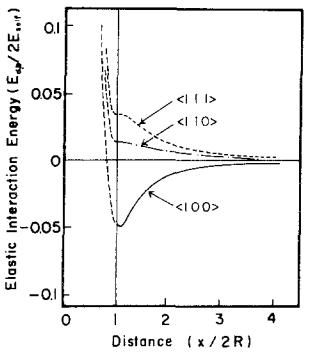

Figure 11 Relationships between the normalized elastic interaction energies and distance from centre-to-centre of two identical spherical particles along the symmetrical three directions, calculated by Yamauchi and co-worker [24].

Therefore, the interaction energy is about same magnitude as the amounts of the total energy change with aspect ratio, because this exists over a range of 10% at most, as seen in Figs. 7 to 10. It is easily understood from Fig. 11 that the sphere inclusions under the strong elastic interaction should be most stable in the "simple cubic structure arrangement". However, whether such an ideal arrangement is formed or not seems to be dependent on the volume fraction of the γ' phase. If the volume fraction of inclusions is not large amount enough to assign the inclusions to every lattice site of the simple cubic structure, the inclusions may not be uniformly arrayed, but locally aligned to reduce the total elastic interaction energy. For such a uniform arrangement the volume fraction is required to be 42% from the geometry of the lattice structure. The present alloy, however, includes only about 27% volume fraction γ' precipitates, estimated from the phase disgram [13]. This value is somewhat less than the ideal one, so that the cuboidal γ' precipitates should be forced to be locally congregated into rows along the ⟨1 0 0⟩ cube directions. Such rows of γ' are clearly observed in Fig. 1. When the aligned cuboids increase in size through Ostwald ripening, the cuboids are considered to change to rods rather than to plates provided that no significant difference exists in the strain-energetic superiority between the rod and plate, because rods may be kinetically produced easier than plates from the cuboids in the rows. Such a shape transformation has clearly been recognized in the experimental work of Chellman *et al.* [26], where the coarsening behaviour of γ' precipitates in Ni–Al alloys containing various percentages of Al were examined. According to their photographs, the cuboidal γ' particles in the higher Al-content alloy maintain their original shape during further annealing and rods were never observed even if the size of the particles increased. On the other hand, the cuboids in the lower alloy transform to rods, keeping their alignment parallel to the ⟨1 0 0⟩ direction. These experimental facts seem to be good evidence of the subsidiary mechanism described above. As shown in Fig. 10, the plate-like precipitates are always energetically more favourable than rods throughout growth, when compression-annealing is involved. However, the cuboidal γ' may transform at first to rods rather than to plates for the reasons discussed above, even if the energetic priority of the plate is slightly higher than that of the rod. To date, the interaction energy has been understood to be related only to the arrangement of inclusions. Nevertheless, the subsidiary influence of the interaction energy on shape transformation should be considered.

6. Conclusions

The influence of external stresses on the morphological changes of γ' precipitates during coarsening in an Ni–15 at.% Al single crystal were investigated, and theoretical evaluation of the energetically favourable shape and its preferred orientation were derived based upon anisotropic elasticity theory.

The shape transformation with growth in size is experimentally obtained to be cuboid → rod → plate, in all the annealing conditions, i.e. compression-annealing, tension-annealing and external stress-free annealing. The external stresses along the [0 0 1] cube direction give preferential orientation to such microstructures; the tension aligns the rods and plates along the [0 0 1] direction parallel to the axis, while compression aligns them along the [1 0 0] and [0 1 0] directions perpendicular to the stress axis. Theoretical evaluation, based upon the anisotropic elasticity theory, of the energetically favourable shapes and orientations of γ', are consistent with experimental results except for the appearence of rods for the compression-annealing. This discrepancy is understood by the conception of shape transformation being controlled not only by energetics in the elastic strain and interfacial energies, but also by the subsidiary influence of the elastic interaction energy.

Acknowledgement

The authors are grateful to Mr T. Kozakai for technical assistance throughout the course of the investigation.

References

1. Y. NAKADA and W. C. LESLIE, *Trans. ASM* **60** (1967) 223.
2. J. M. OBIAK and D. F. PAULONIS, *Met. Trans.* **5** (1974) 143.
3. G. SAUTHOFF, *Z. Metalk.* **68** (1977) 500.
4. T. ETO, A. SATO and T. MORI, *Acta Met.* **26** (1978) 499.
5. M. LAUTHAN, *J. Nucl. Mater.* 9 (1963) 170.
6. *Idem, Trans. Met. Soc. AIME* **227** (1963) 1166.
7. J. K. TIEN and S. M. COPLEY, *Met. Trans* **2** (1971) 215, 543.
8. A. PINEAU, *Acta Met.* **24** (1976) 550.
9. J. D. ESHELBY, *Prog. Solid. Mech.* **2** (1961) 89.
10. *Idem, Proc. Roy. Soc. A* **241** (1957) 376.
11. E. HORNBOGEN and M. ROTH, *Z. Metalk.* **58** (1967) 842.
12. R. G. DAVIES and N. S. STOLOFF, *Trans. AIME* **233** (1965) 714.
13. R. O. WILLIAMS, *ibid* **215** (1959) 1026.
14. J. KAGAWA, T. MIYAZAKI and H. MORI, *Trans. Japan Inst. Metals* **18** (1977) 707.
15. A. CHOU, A. DATTA, G. H. MEIER and W. A. SOFFA, *J. Mater. Sci.* **13** (1978) 541.
16. K. ONO and R. STERN, *Trans. Met. Soc. AIME* **245** (1969) 171.
17. H. B. HONTINGTON, *Solid Stat. Phys.* **7** (1958) 265.
18. N. KINOSHITA and T. MURA, *Phys. Stat. Sol. (a)* **5** (1971) 759.
19. S. C. LIN and T. MURA, *ibid* **15** (1973) 281.
20. J. K. LEE and D. M. BARNETT, *Met. Trans.* **8A** (1977) 96.
21. A. J. ARDELL, *Acta Met.* **16** (1968) 511.
22. C. L. COREY and B. LISOWSKY, *Trans. Met Soc. AIME*, **239** (1967) 239.
23. A. G. KHACHATURYAN, *Phys. Stat. Sol. (a)* **26** (1974) 61.
24. H. YAMAUCHI, *Busseiken-dayori* **14** (1974) 24 (in Japanese).
25. H. YAMAUCHI and D. de FONTAINE, (to be published).
26. D. CHELLMAN and A. J. ARDELL, *Acta Met.* **22** (1974) 577.

Received 31 July 1978 and accepted 5 January 1979.